



ISTITUTO ITALIANO  
DI TECNOLOGIA  
DYNAMIC LEGGED SYSTEMS

arXiv:2101.02279v1 [cs.RO] 6 Jan 2021

# On State Estimation for Legged Locomotion over Soft Terrain

Shamel Fahmi, Geoff Fink, and Claudio Semini

**Accepted on:** January, 2021.

**Published in:** IEEE Sensors Letters

**To cite this paper:**

---

S. Fahmi, G. Fink, C. Semini, "On State Estimation for Legged Locomotion over Soft Terrain," *IEEE Sensors Letters*, 2021.

---

For this and other publications from the Dynamic Legged Systems lab (DLS):  
<https://dls.iit.it/dls-publications>

©2021 IEEE. Personal use of this material is permitted. Permission from IEEE must be obtained for all other uses, in any current or future media, including reprinting/republishing this material for advertising or promotional purposes, creating new collective works, for resale or redistribution to servers or lists, or reuse of any copyrighted component of this work in other works.

## On State Estimation for Legged Locomotion over Soft Terrain

Shamel Fahmi<sup>\*</sup>, Geoff Fink<sup>\*\*</sup>, and Claudio Semini<sup>\*\*</sup>

*Dynamic Legged Systems lab, Istituto Italiano di Tecnologia (IIT), Genova, Italy.*

<sup>\*</sup>Student Member, IEEE      <sup>\*\*</sup>Member, IEEE

Manuscript received XXXX; revised XXXX; accepted XXXX. Date of publication XXXX; date of current version XXXX.

**Abstract**—Locomotion over soft terrain remains a challenging problem for legged robots. Most of the work done on state estimation for legged robots is designed for rigid contacts, and does not take into account the physical parameters of the terrain. That said, this letter answers the following questions: how and why does soft terrain affect state estimation for legged robots? To do so, we utilized a state estimator that fuses IMU measurements with leg odometry that is designed with rigid contact assumptions. We experimentally validated the state estimator with the HyQ robot trotting over both soft and rigid terrain. We demonstrate that soft terrain negatively affects state estimation for legged robots, and that the state estimates have a noticeable drift over soft terrain compared to rigid terrain.

**Index Terms**—State Estimation, Legged Robots, Soft Contacts

### I. INTRODUCTION

Quadruped robots are advancing towards being fully autonomous as can be seen by their recent development in research and industry, and their remarkable agile capabilities [1]–[3]. This demands quadruped robots to be robust while traversing a wide variety of unexplored complex non-flat terrain. The terrain may not just vary in geometry, but also in its physical properties such as terrain impedance or friction. Reliable state estimation is a major aspect for the success of the deployment of quadruped robots because most locomotion planners and control strategies rely on an accurate estimate of the pose and velocity of the robot. Furthermore, reliable state estimation is essential, not only for locomotion (low-level state estimation), but also for autonomous navigation and inspection tasks that are emerging applications for quadruped robots (task-level state estimation).

To date, most of the work done on state estimation for legged robots are based on filters that fuse multiple sensor modalities. These sensor modalities mainly include high frequency inertial measurements and kinematic measurements (e.g., leg odometry), as well as other low frequency modalities (e.g., cameras and lidars) to correct the drift.

For instance, an extended Kalman filter (EKF)-based sensor fusion algorithm has been proposed by [4] that fuses IMU measurements, leg odometry, stereo vision, and lidar. In [5], a similar algorithm has been proposed that fuses IMU measurements, leg odometry, stereo vision, and GPS. In [2], a nonlinear observer that fuses IMU measurements and leg odometry has been proposed. In [6], a state estimator fuses a globally exponentially stable (GES) nonlinear attitude observer based on IMU measurements with leg odometry to provide bounded velocity estimates. The global stability is important for cases when the robot may have fallen over whereas typical EKF-based works may diverge. The bounded velocity estimates help to decrease drift in the unobservable position estimates. Finally, an approach similar to [6] has been proposed in [7]. This approach proposed an invariant

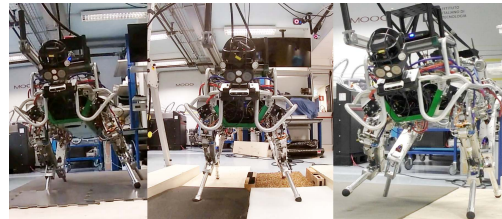


Fig. 1. HyQ traversing multiple terrains of different compliances.

EKF-based sensor fusion algorithm that includes IMU measurements, contact sensor dynamics, and leg odometry.

The aforementioned state estimators are shown to be reliable on stiff terrain. Yet, over soft terrain (as shown in Fig. 1), the performance of these state estimators starts to decline. Over soft terrain, the state estimator has difficulties determining when a foot is in contact with the ground. For instance, the state estimator has difficulties determining if the foot is in the air, if the foot is applying more force than the terrain (terrain compression), if the terrain itself is applying more force than the foot (terrain expansion), or if the foot and the terrain are applying the same force (rigid terrain). This results in a large position estimate drift, and it was reported in our previous work [8] where we noted that we encountered difficulties because of state estimation over soft terrain. Apart from our previous work, other works also mention that state estimation over soft terrain is a challenging task, e.g., [9], [10]. Yet, to the authors' knowledge, literature has not yet discussed the question on how soft terrain affects the state estimation.

The contributions of this work are the experimental analysis and formal study on: the effects of soft terrain on state estimation, the reasons behind these effects, and simple ways to improve state estimation. This letter is building upon our previous work on soft terrain adaptation [8] and on state estimation [6].

The rest of this letter is organized as follows: Section II describes the robot model, the onboard sensors, and how to estimate the ground reaction forces (GRFs) acting on the robot. Section III explains the state estimator used in this letter, and how to estimate the base velocity of the robot using leg odometry. Section IV details the results of our experiment and demonstrates how soft terrain affects state estimation. Finally, Section V presents our conclusions.

Corresponding author: Shamel Fahmi (e-mail: shamel.fahmi@iit.it).

Associate Editor: XXXX XXXX.

Digital Object Identifier 10.1109/LENS.20XX.0000000

## II. MODELING, SENSING, AND ESTIMATING

In this letter, we consider the quadruped robot HyQ [11] shown in Fig. 1. Each leg has three actuated joints. Despite experimenting on a specific platform, the problem is generic in nature and it applies equally to any legged robot. Furthermore, by using the 90 kg HyQ robot, a heavy and strong platform, we are exciting more dynamics.

We introduce the following reference frames: the body frame  $\mathcal{B}$  which is located at the geometric center of the trunk (robot torso), and the navigation frame  $\mathcal{N}$  which is assumed inertial (world frame). The basis of the body frame are orientated forward, left, and up. To simplify notation, the IMU is located such that the accelerometer measurements are directly measured in  $\mathcal{B}$ .

**Kinematics and Dynamics.** Assuming that all of the external forces are exerted on the feet, the dynamics of the robot is

$$M(\bar{x})\ddot{\bar{x}} + h(\bar{x}, \dot{\bar{x}}) = \bar{\tau} \quad (1)$$

where  $\bar{x} = [x^T \ \eta^T \ q^T]^T \in \mathbb{R}^{18}$  is the generalized robot states,  $\dot{\bar{x}} \in \mathbb{R}^{18}$  is the corresponding generalized velocities,  $\ddot{\bar{x}} \in \mathbb{R}^{18}$  is the corresponding generalized accelerations,  $x \in \mathbb{R}^3$  is the position of the base,  $\eta \in \mathbb{R}^3$  is the attitude of the base,  $q \in \mathbb{R}^{12}$  is the vector of joint angles of the robot,  $M \in \mathbb{R}^{18 \times 18}$  is the joint-space inertia matrix,  $h$  is the vector of Coriolis, centrifugal and gravity forces,  $\bar{\tau} = ([0 \ \tau^T]^T - JF) \in \mathbb{R}^{18}$ ,  $\tau \in \mathbb{R}^{12}$  is the vector of actuated joint torques,  $J \in \mathbb{R}^{18 \times 12}$  is the floating base Jacobian, and  $F \in \mathbb{R}^{12}$  is the vector of external forces (i.e., GRFs).

We solve for the GRFs  $F_\ell$  of each leg  $\ell$  using the actuated part of the dynamics in (1).

$$F_\ell = -\alpha_\ell (J_\ell^T(q_\ell))^{-1} (\tau_\ell - h_\ell(\bar{x}_\ell, \dot{\bar{x}}_\ell)) \quad (2)$$

$F_\ell \in \mathbb{R}^3 \subset C$  is the GRFs for  $\ell$  in  $\mathcal{B}$ ,  $J_\ell \in \mathbb{R}^{3 \times 3} \subset J$  is the foot Jacobian of  $\ell$ ,  $\tau_\ell \in \mathbb{R}^3 \subset \tau$  is the vector of joint torques of  $\ell$ ,  $h_\ell \in \mathbb{R}^3 \subset h$  is the vector of centrifugal, Coriolis, gravity torques of  $\ell$  in  $\mathcal{B}$ , and  $\alpha_\ell \in \{0, 1\}$  selects if the foot is on the ground or not. A threshold of  $F_\ell$  is typically used to calculate  $\alpha_\ell$ .

$$\alpha_\ell = \begin{cases} 1 & \|(J_\ell^T)^{-1}(\tau_\ell - h_\ell)\| > \epsilon \\ 0 & \text{otherwise} \end{cases} \quad (3)$$

where  $\epsilon > 0 \in \mathbb{R}$  is the threshold.

*Assumption 1:* There exists a force threshold  $\epsilon$  that determines if the foot is in contact with the environment.

The translational and rotational kinematics, and the translational dynamics of the robot as a single rigid body in  $\mathcal{N}$  are

$$\dot{x}^n = v^n \quad \dot{v}^n = a^n + g^n \quad \dot{R}_b^n = R_b^n S(\omega^b) \quad (4)$$

where  $x^n \in \mathbb{R}^3$ ,  $v^n \in \mathbb{R}^3$ ,  $a^n \in \mathbb{R}^3$  are the position, velocity, and acceleration of the base in  $\mathcal{N}$ , respectively,  $R_b^n \in \text{SO}(3)$  is the rotation matrix from  $\mathcal{B}$  to  $\mathcal{N}$ , and  $\omega^b$  is the angular velocity of the base in  $\mathcal{B}$ . The skew symmetric matrix function is  $S(\cdot)$ .

**Sensors.** The modeling assumes that the quadruped robot is equipped with a six-axis IMU on the trunk (3 Degrees of Freedom (DoFs) gyroscope and 3 DoFs accelerometer), and that every joint contains an encoder and a torque sensor. The accelerometer measures specific force  $f_s^b \in \mathbb{R}^3$

$$f_s^b = a^b + g^b \quad (5)$$

where  $a^b \in \mathbb{R}^3$  is the acceleration of the body in  $\mathcal{B}$  and  $g^b \in \mathbb{R}^3$  is the acceleration due to gravity in  $\mathcal{B}$ . The gyroscope directly measures angular velocity  $\omega^b \in \mathbb{R}^3$  in  $\mathcal{B}$ . The encoders are used to measure

the joint position  $q_i \in \mathbb{R}$  and joint speed  $\dot{q}_i \in \mathbb{R}$ . The pose of each joint (i.e., the forward kinematics) is assumed to be exactly known. The torque sensors in the joints directly measure torque  $\tau_i \in \mathbb{R}$ .

The measured values of all of the sensors differ from the theoretical values in that they contain a bias and noise:  $\tilde{x} = x + b_x + n_x$  where  $\tilde{x}$ ,  $b_x$ , and  $n_x$  are the measured value, bias, and noise of  $x$ , respectively. All of the biases are assumed to be constant or slowly time-varying, and all of the noise variables have zero mean and a Gaussian distribution.

## III. STATE ESTIMATOR

To compare the effect of different terrains, we use the state-of-the-art low-level state estimator from [6]. It includes input from three proprioceptive sensors: an IMU, encoders, and torque sensors. For reliability and speed no exteroceptive sensors are used. The state estimator consists of three major components: an attitude observer, leg odometry, and a sensor fusion algorithm.

**Non-linear Attitude Observer.** Typically in the quadruped robot literature an EKF is used for attitude estimation, e.g., [4], [5], [12]. However, our *attitude observer* [6] is GES, and it consists of a *non-linear observer (NLO)* [13] and an *eXogeneous Kalman Filter (XKF)* [14]. The NLO is

$$\begin{aligned} \dot{\hat{R}}_b^n &= \hat{R}_b^n S(\omega^b - \hat{b}^b) + \sigma K_p J_s(\hat{R}_b^n) \\ \hat{b}^b &= \text{Proj}(\hat{b}^b, -k \text{vex}(\mathbb{P}(\hat{R}_{bs}^{nT} K_p J_s(\hat{R}_b^n)))) \\ J_s(\hat{R}_b^n) &= \sum_{j=1}^k (y_j^n - \hat{R}_{bs}^n y_j^b) y_j^{bT} \end{aligned} \quad (6)$$

where  $K_p \in \mathbb{R}^{3 \times 3}$  is a symmetric positive-definite gain matrix,  $k > 0 \in \mathbb{R}$  is a scalar gain,  $\sigma \geq 1 \in \mathbb{R}$  is a scaling factor,  $\hat{R}_{bs}^n = \text{sat}(\hat{R}_b^n)$ , the function  $\text{sat}(X)$  saturates every element of  $X$  to  $\pm 1$ ,  $\text{Proj}$  is a parameter projection that ensures that  $\|\hat{b}\| < M_b$ ,  $M_b > 0 \in \mathbb{R}$  is a constant known upper bound on the gyro bias,  $\mathbb{P}(X) = \frac{1}{2}(X + X^T)$  for any square matrix  $X$ , and  $J_s$  is the stabilizing injection term. The observer is GES for all initial conditions assuming there exists  $k > 1$  non-collinear vector measurements, i.e.,  $|y_i^n \times y_j^n| > 0$  where  $i, j \in \{1, \dots, k\}$ . Furthermore, if there is only one measurement the observer is still GES if the following persistency of excitation (PE) condition holds: if there exist constants  $T > 0 \in \mathbb{R}$  and  $\gamma > 0 \in \mathbb{R}$  such that, for all  $t \geq 0$ ,  $\int_t^{t+T} y_1^n(\tau) y_1^n(\tau)^T d\tau \geq \gamma I$  holds then  $y_1^n$  is PE. See [13] for proof.

The XKF [14] is similar to an EKF in that it linearizes a nonlinear model about an estimate of the state and then applies the typical linear time-varying (LTV) Kalman filter (KF) to the linearized model. If the estimate is close to the true state then the filter is near-optimal. However, if the estimate is not close to the true state, the filter can quickly diverge. To overcome this problem, the XKF linearizes about a globally stable exogenous signal from a NLO. The cascaded structure maintains the global stability properties from the NLO and the near-optimal properties from the KF. The observer is

$$\begin{aligned} \dot{\hat{x}} &= f_x + C(\hat{x} - \tilde{x}) + K(z - h_x - H(\hat{x} - \tilde{x})) \\ \dot{P} &= CP + PC^T - KHP + Q \\ K &= PH^T R^{-1} \end{aligned} \quad (7)$$

where  $C = \partial f_x / \partial x|_{\tilde{x}, u}$ ,  $H = \partial h_x / \partial x|_{\tilde{x}, u}$ ,  $\tilde{x} \in \mathbb{R}^n$  is the bounded estimate of  $x$  from the globally stable NLO. See [14] for the stability proof.

**Leg Odometry.** Leg odometry computes the overall base velocity  $\dot{x}^b$  of the robot by combining the contribution of each foot velocity  $\dot{x}_\ell^b$ . Each leg  $\ell$  only contributes to the leg odometry when it is in contact  $\alpha_\ell$ . Thus, we calculate the overall base velocity  $\dot{x}^b$  as

$$\dot{x}_\ell^b = -\alpha_\ell (J_\ell(q_\ell)\dot{q} - \omega^b \times x_\ell^b) \quad \dot{x}^b = \frac{1}{n_s} \sum_\ell \dot{x}_\ell^b \quad (8)$$

where  $n_s = \sum \alpha_\ell$  is the number of stance legs.

*Assumption 2:* The leg odometry assumes that the robot is always in rigid contact with the terrain. This implies that the stance feet do not move in  $\mathcal{N}$ , there is no slippage, the terrain does not expand or compress, and the robot does not jump or fly.

**Sensor Fusion.** Lastly, the inertial measurements (5) are fused with the leg odometry (8). The main advantage of decoupling the attitude from the position and linear velocity is that the resulting dynamics is LTV, and thus has guaranteed stability properties. i.e., the filter will not diverge in finite time.

We use a LTV KF with the dynamics (4), the accelerometer (5), and leg odometry (8).

$$\begin{aligned} \dot{\hat{x}} &= f_{\hat{x}} + \underline{K}(z - h_{\hat{x}}) \\ \dot{\underline{P}} &= \underline{CP} + \underline{PC}^T - \underline{KHP} + \underline{Q} \\ \underline{K} &= \underline{PH}^T \underline{R}^{-1} \end{aligned} \quad (9)$$

where the state  $\hat{x} = [x^{nT} \quad v^{nT}]^T \in \mathbb{R}^6$  is position and velocity of the base, the input  $u = (R_b^n f_s^b - g^n) \in \mathbb{R}^3$  is the acceleration of the base, the measurement  $z = R_\ell^n x_\ell^b \in \mathbb{R}^3$  is the leg odometry,  $\underline{K} \in \mathbb{R}^{6 \times 3}$  is the Kalman gain,  $\underline{P} \in \mathbb{R}^{6 \times 6}$  is the covariance matrix,  $\underline{Q} \in \mathbb{R}^{6 \times 6}$  is the process noise and  $\underline{R} \in \mathbb{R}^{3 \times 3}$  is the measurement noise covariance, and

$$f_{\hat{x}} = \begin{bmatrix} v^n \\ u \end{bmatrix} \quad \underline{C} = \begin{bmatrix} 0_3 & I_3 \\ 0_3 & 0_3 \end{bmatrix} \quad \underline{H} = [0_3 \quad I_3]$$

and  $I_3$  and  $0_3$  are the  $3 \times 3$  identity matrix and matrix of all zeros, respectively.

## IV. EXPERIMENTAL RESULTS

To analyze the differences in state estimation between rigid and soft terrain, we used HyQ and our state estimator. HyQ has twelve torque-controlled joints powered by hydraulic actuators. HyQ has three types of on board proprioceptive sensors: joint encoders, force/torque sensors, and IMUs. Every joint has an absolute and a relative encoder to measure the joint angle and speed. The absolute encoder (AMS Programmable Magnetic Rotary Encoder - AS5045) measures the joint angle when the robot is first turned on, while the relative encoder (Avago Ultra Miniature, High Resolution Incremental Encoder - AEDA-3300-TE1) measures how far the joint has moved at every epoch. Every joint contains a force or torque sensor. Two joints have a load cell (Burster Subminiature Load Cell - 8417-6005) and one joint has a custom designed torque sensor based on strain-gauges. In the trunk of the robot there is a fibre optic-based, military grade KVH 1775 IMU.

We used the state estimator (6)-(9) on the *Soft Trot in Place* and the *Rigid Trot in Place* dataset from the dataset published in [15]. HyQ was manually controlled to trot on a foam block of  $160 \times 120 \times 20$  cm, and on a rigid ground. An indentation test of the foam shows the foam has an average stiffness of 2400 N/m. All of the sensors were

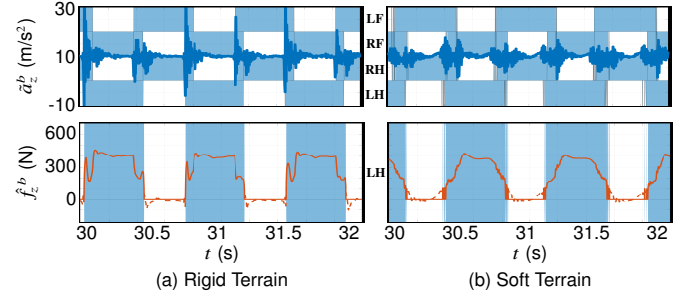


Fig. 2. The  $z$  component of the measured specific force  $\hat{a}_z^b$  (top), and the estimated ground reaction forces  $\hat{f}_z^b$  (bottom), in the body frame  $\mathcal{B}$  of HyQ during a trotting experiment. The highlighted regions show when the given foot is in stance, and the feet are denoted as left-front (LF), right-front (RF), left-hind (LH), and right-hind (RH).

recorded at 1000 Hz. A motion capture system (MCS) recorded the ground truth data with millimetre accuracy at 250 Hz.

The experiments confirmed our original hypothesis that soft terrain negatively impacts state estimation and also allowed us to investigate why. It is important to note that rigid versus soft terrain had no impact on the attitude estimation. For space reasons, all attitude plots have been omitted.

The first distinct difference between soft and rigid terrain is the specific force measurement of the body as seen in Fig. 2. On the rigid terrain there are large impacts and then vibrations every time a foot touches down. Whereas the soft terrain damped out these vibrations. Next, on the soft terrain more prolonged periods of positive and negative acceleration can be seen. This acceleration can also be seen in the plots of the GRFs in Fig. 2 where the GRFs on the soft terrain are more continuous when compared to the rigid terrain. In other words, there are longer loading and unloading phases.

The most important differences between soft and rigid terrain are seen in the velocity and position estimates as shown in Fig. 3. We can see that the leg odometry has large erroneous peaks in  $z$  velocity at both touch-down and lift-off. These peaks in velocities can then be seen in the position estimates as a drift. On the other hand, the  $x$  and  $y$  position estimates are quite accurate and only have a slow drift.

In the figures, we can also see multiple of the state estimators assumptions being broken. First, there does not exist a constant  $\epsilon$  that can describe when the foot is in contact with the ground, which is contradicting Assumption 1. The contact  $\epsilon$  is no longer binary (i.e., supporting/not-supporting the weight of the robot), but the contact is now a continuous value with varying amounts of the robot's weight being supported and sometimes even pushed. When trying to use the previous simple model, the contact ignores a large portion of the loading and unloading phase. Furthermore, it often chatters rapidly between contact/non-contact when the force is close to  $\epsilon$ . Second, the foot is moving for almost the entire contact (i.e., non-zero acceleration) on soft terrain as shown in Fig. 2. This contradicts Assumption 2 that the foot velocity is zero when in contact. Third, (8) is broken. It assumes that all of the velocity (and all of the acceleration) is a result of the GRFs, but not all of the acceleration due to gravity is being accounted for. Hence, the robot appears to drift up and away from the ground.

There are a few simple ways to try to improve the estimates of this or other similar state estimators. The first is to tune  $\epsilon$  in (3). By increasing  $\epsilon$  there would be less erroneous velocity, but in doing so it would also ignore part of the leg odometry. In general, on a planar

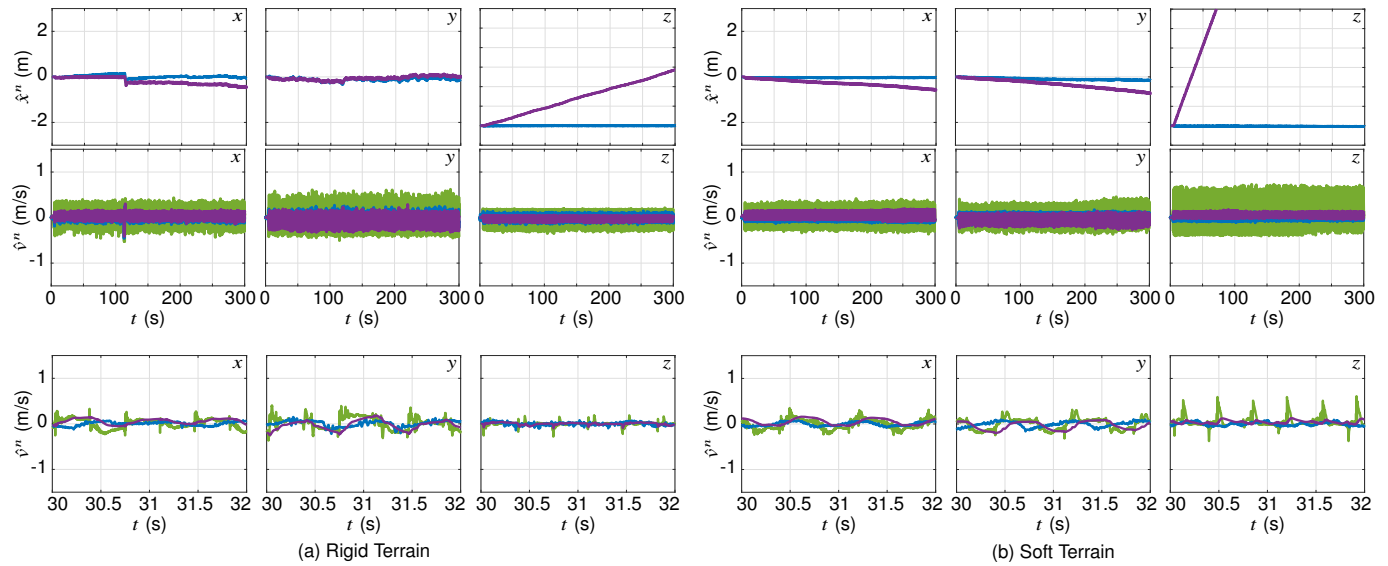


Fig. 3. The estimated trunk position  $\hat{x}^n$  (top), and the estimated trunk velocity  $\hat{v}^n$  (middle and bottom), in the navigation frame  $\mathcal{N}$  of HyQ during a trotting experiment using sensor fusion (purple) versus the raw leg odometry (green), and the motion capture system (blue). The first two rows show the full experiment ( $0 \leq t \leq 300$ ) s and the bottom row is zoomed in ( $30 \leq t \leq 32$ ) s.

surface, a reduced drift in the  $z$  direction comes at the cost of an increased error in the  $x$  and  $y$  directions. A second method could be to have an adaptive velocity bias for the leg odometry. However, the bias is not constant and it depends on both the gait and the terrain. Thus, the problem of estimating the body velocity of the robot using leg odometry remains open.

## V. CONCLUSIONS

In this letter, we present an experimental validation and a formal study on the influence of soft terrain on state estimation for legged robots. We utilized a state-of-the-art state estimator that fuses IMU measurements with leg odometry. We experimentally analyzed the differences between soft and rigid terrain using our state estimator and a dataset of the HyQ robot. That said, we report three main outcomes. First, we showed that soft terrain results in a larger drift in the position estimates, and larger errors in the velocity estimates compared to rigid terrain. These problems are caused by the broken legged odometry contact assumptions on soft terrain. Second, we also showed that over soft terrain, the contact with the terrain is no longer binary and it often chatters rapidly between contact and non-contact. Third, we showed that soft terrain affects many states besides the robot pose. This includes the contact state and the GRFs which are essential for the control of legged robots. Future works include extending the state estimator to incorporate the terrain impedance in the leg odometry model. Additionally, further datasets will be recorded to investigate the long-term drift in the forward and lateral directions.

## REFERENCES

- C. Semini, V. Barasuol, M. Focchi, C. Boelens, M. Emara, S. Casella, O. Villarreal, R. Orsolino, G. Fink, S. Fahmi, G. Medrano-Cerda, and D. G. Caldwell, "Brief introduction to the quadruped robot HyQReal," in *Italian Conference on Robotics and Intelligent Machines (I-RIM)*, Rome, Oct. 2019, pp. 1–2.
- G. Bleidt, M. J. Powell, B. Katz, J. Di Carlo, P. M. Wensing, and S. Kim, "MIT Cheetah 3: Design and control of a robust, dynamic quadruped robot," in *Int. Conf. on Intell. Robots and Syst. (IROS)*, Madrid, Spain, Oct. 2018, pp. 2245–2252, DOI:10.1109/IROS.2018.8593885.
- M. Raibert, K. Blankespoor, G. Nelson, and R. Playter, "BigDog, the rough-terrain quadruped robot," *IFAC Proceedings Volumes*, vol. 41, no. 2, pp. 10822–10825, 2008, DOI:10.3182/20080706-5-KR-1001.01833.
- S. Nobili, M. Camurri, V. Barasuol, M. Focchi, D. Caldwell, C. Semini, and M. Fallon, "Heterogeneous sensor fusion for accurate state estimation of dynamic legged robots," in *Proc. of Robot.: Sci. and Syst. (RSS)*, Cambridge, Massachusetts, Jul. 2017, pp. 1–9, DOI:10.15607/RSS.2017.XIII.007.
- J. Ma, M. Bajracharya, S. Susca, L. Matthies, and M. Malchano, "Real-time pose estimation of a dynamic quadruped in GPS-denied environments for 24-hour operation," *Int. J. of Robotics Res.*, vol. 35, no. 6, pp. 631–653, 2016, DOI:10.1177/0278364915587333.
- G. Fink and C. Semini, "Proprioceptive sensor fusion for quadruped robot state estimation," in *IEEE/RSJ International Conference on Intelligent Robots and Systems (IROS)*, Las Vegas, Nevada, Oct. 2020, pp. 1–7.
- R. Hartley, M. Ghaffari, R. M. Eustice, and J. W. Grizzle, "Contact-aided invariant extended Kalman filtering for robot state estimation," *Int. J. of Robotics Res.*, vol. 39, no. 4, pp. 402–430, 2020, DOI:10.1177/0278364919894385.
- S. Fahmi, M. Focchi, A. Radulescu, G. Fink, V. Barasuol, and C. Semini, "STANCE: Locomotion Adaptation over Soft Terrain," *IEEE Transactions on Robotics*, vol. 36, no. 2, pp. 443–457, 2020, DOI:10.1109/TRO.2019.2954670.
- D. Wisth, M. Camurri, and M. Fallon, "Preintegrated velocity bias estimation to overcome contact nonlinearities in legged robot odometry," in *2020 IEEE International Conference on Robotics and Automation (ICRA)*, 2020, pp. 392–398, DOI:10.1109/ICRA40945.2020.9197214.
- B. Henze, R. Balachandran, M. A. Roa-Garzón, C. Ott, and A. Albu-Schäffer, "Passivity analysis and control of humanoid robots on movable ground," *IEEE Robot. Automat. Lett. (RA-L)*, vol. 3, no. 4, pp. 3457–3464, Oct. 2018, DOI:10.1109/LRA.2018.2853266.
- C. Semini, N. G. Tsagarakis, E. Guglielmino, M. Focchi, F. Cannella, and D. G. Caldwell, "Design of HyQ – a hydraulically and electrically actuated quadruped robot," *Proc. Inst. Mech. Eng. I J. Syst. Control Eng.*, vol. 225, no. 6, pp. 831–849, 2011, DOI:10.1177/0959651811402275.
- M. Bloesch, C. Gehring, P. Fankhauser, M. Hutter, M. A. Hoepflinger, and R. Siegwart, "State estimation for legged robots on unstable and slippery terrain," in *Int. Conf. on Intell. Robots and Syst. (IROS)*, Tokyo, Japan, Nov. 2013, pp. 6058–6064, DOI:10.1109/IROS.2013.6697236.
- H. F. Grip, T. I. Fossen, T. A. Johansen, and A. Saberi, "Globally exponentially stable attitude and gyro bias estimation with application to GNSS/INS integration," *Automatica*, vol. 51, pp. 158–166, 2015, DOI:10.1016/j.automatica.2014.10.076.
- T. A. Johansen and T. I. Fossen, "The eXogenous Kalman Filter (XKF)," *Int. J. Control*, vol. 90, no. 2, pp. 161–167, 2017, DOI:10.1080/00207179.2016.1172390.
- G. Fink, *Proprioceptive Sensor Dataset for Quadruped Robots*. IEEE Dataport, 2019, DOI:10.21227/4vxz-xw05.